Chapter 8
Some Optimization Problems

Abstract In this chapter, the problems of safety analysis and optimization of a moving elastic plate travelling between two rollers at a constant axial velocity are considered. We will use a model of a thin elastic plate subjected to bending and in-plane tension (distributed membrane forces). We will study transverse buckling (divergence) of the plate and its brittle and fatigue fracture caused by fatigue crack growth under cyclic in-plane tension (loading). Our aim is to find the safe ranges of velocities of an axially moving plate analytically under the constraints of longevity and stability. In the end of this chapter, the expressions for critical buckling velocity and the number of cycles before the fracture (longevity of the plate) as a function of in-plane tension and other problem parameters are used for formulation and we will study the case as an optimization problem. Our target is to find the optimal in-plane tension to maximize the performance function of paper production. This problem is solved analytically and the obtained results are presented as formulae and numerical tables.

8.1 Optimization of Moving Plates Subjected to Instability and Fracture

It is known that, in systems with travelling continuum, an increase in tension has a stabilizing effect but a decrease in tension may lead to a loss of stability. From the viewpoint of fracture, tension has an opposite effect: high tension may lead to growing or arising of cracks, and tension low enough then guarantees safe conditions. In practice, both instability and material fracture may lead to web breaks.

In this section, we will present constraints for the plate velocity and the structural longevity so that the considered system would perform in a safe manner. By longevity

---

Co-author in this chapter: Maria Tirronen, Department of Mathematical Information Technology, University of Jyväskylä.
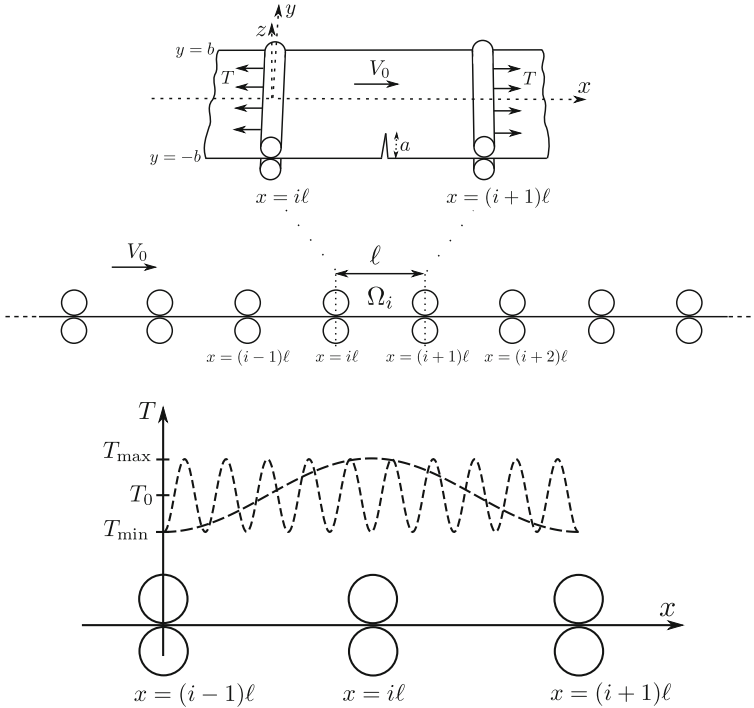
Fig. 8.1 *Top* A plate travelling through a system of supporting rollers, and having an initial crack. *Bottom* Examples of cyclic tension. There may be few or many tension cycles per span. (Reproduced from Banichuk et al. 2013)

or structural longevity, we refer to the number of cycles that the (cracked) material sustains before fracture failure. We will also construct a productivity function, with the help of which an optimal value for in-plane tension will be sought.

8.1.1 Optimization Criterion and Constraints

Consider an elastic plate travelling at a constant velocity V_0 in the x direction and being simply supported by a system of rollers located at $x = 0$, ℓ, 2ℓ, 3ℓ, ... (Fig. 8.1). A rectangular element Ω_i, $i = 0, 1, 2, \ldots$, of the plate

$$\Omega_i \equiv \left\{ (x, y) \in \mathbb{R}^2 \mid i\ell < x < (i+1)\ell, \; -b < y < b \right\} \qquad (8.1)$$

is considered in a cartesian coordinate system, where ℓ and b are prescribed geometric parameters. Additionally, assume that the considered plate is represented as an isotropic elastic plate having constant thickness h, Poisson ratio ν, Young modulus

E, and bending rigidity D. The plate elements in (8.1) have small initial cracks (Fig. 8.1) of length a with a given upper bound a_0, i.e.,

$$0 < a \leq a_0 , \tag{8.2}$$

and are subjected to homogeneous tension T, acting in the x direction.

The sides of the plate element ($i = 1, 2, 3, \dots$)

$$\{ x = i\ell, \quad -b \leq y \leq b \} \quad \text{and} \quad \{ x = (i + 1)\ell, \quad -b \leq y \leq b \}$$

are simply supported and the sides

$$\{ y = -b, \quad i\ell \leq x \leq (i + 1)\ell \} \quad \text{and} \quad \{ y = b, \quad i\ell \leq x \leq (i + 1)\ell \}$$

are free of tractions.

Consider the following scenario, where the plate is moving under cyclic in-plane tension and fatigue crack growth is realised. Suppose that the plate is subjected to a cyclic tension T that varies in the given limits

$$T_{\min} \leq T \leq T_{\max} ,$$

where

$$T_{\min} = T_0 - \Delta T , \qquad T_{\max} = T_0 + \Delta T .$$

Above, $\Delta T > 0$ is a given parameter such that

$$T_0 - \Delta T > 0 \quad \text{and} \quad \frac{\Delta T}{T_0} \ll 1 . \tag{8.3}$$

For one cycle, the tension increases from $T = T_{\min}$ up to $T = T_{\max}$ (the loading process) and then decreases from $T = T_{\max}$ to $T = T_{\min}$ (the unloading process). The loading and unloading processes are supposed to be quasistatic; dynamical effects are excluded.

The product of the plate velocity V_0 and the process time t_f can be considered a productivity criterion (performance function), i.e.,

$$J = m_0 V_0 t_f , \qquad m_0 = 2bm . \tag{8.4}$$

Here, m is the mass per unit area of the plate. In (8.4), the velocity V_0 is taken from the safe interval

$$0 < V_0 < V_0^{cr} ,$$

where V_0^{cr} is the critical buckling speed.

A safe interval for the safe functioning time (number of cycles) is written as

$$0 < t_f < t_f^{cr} \quad \text{or} \quad 0 < n < n^{cr} ,$$

where t_f^{cr} and n^{cr} are, respectively, the time interval and the total number of cycles before fatigue fracture. For a small cycle time period τ and a big number of cycles n, we assume that $t_f \approx n\tau$. Note that the critical buckling velocity V_0^{cr} and the critical functioning time t_f^{cr} (critical number of cycles n^{cr}) depend on the parameters of the average in-plane tension T_0, and the admissible variance ΔT, i.e

$$V_0^{cr} = V_0^{cr}(T_0, \Delta T) ,$$

$$t_f^{cr} = t_f^{cr}(T_0, \Delta T) ,$$

$$n^{cr} = n^{cr}(T_0, \Delta T) .$$

Consequently, the maximum value of the productivity criterion for the given values T_0 and ΔT is evaluated as

$$J(T_0, \Delta T) = m_0 V_0^{cr}(T_0, \Delta T) t_f^{cr}(T_0, \Delta T)$$

$$= m_0 \tau V_0^{cr}(T_0, \Delta T) n^{cr}(T_0, \Delta T) .$$

The optimal average (mean) in-plane tension T_0 is found by solving the following optimization problem:

$$J^* = \max_{T_0} \ J(T_0, \Delta T) .$$

To solve the formulated optimization problem, we will use the explicit analytical expressions for the values V_0^{cr} and n^{cr}. The value of T_0, giving the maximal production J^*, is denoted by T_0^*.

To evaluate n^{cr}, let us apply fatigue crack growth theory. Suppose that the plate contains one initial crack of length a_0. The process of fatigue crack growth under a cyclic tension (loading) can be described by the following equation (Paris and Erdogan 1963) and initial condition

$$\frac{da}{dn} = C\kappa_0^k a^{k/2} , \tag{8.5}$$

where

$$\kappa_0 = \frac{2\beta\sqrt{\pi}}{h}\Delta T .$$

The variance ΔK of the stress intensity factor K is determined with the help of the formulae

$$\Delta K = K_{\max} - K_{\min}, \qquad K_{\max} = \beta \sigma_{\max} \sqrt{\pi a},$$

$$K_{\min} = \beta \sigma_{\min} \sqrt{\pi a}, \qquad \sigma_{\max} = \frac{T_{\max}}{h}, \qquad \sigma_{\min} = \frac{T_{\min}}{h}. \qquad (8.6)$$

In (8.5), C and k are material constants. In (8.6), h is the thickness of the plate, n is the number of cycles, and $\sigma_{\max}$, $K_{\max}$, $\sigma_{\min}$ and $K_{\min}$ are, respectively, the maximum and minimum values of the stress σ and the stress intensity factor K in any given loading cycle. For the considered case, the surface crack geometric factor is $\beta = 1.12$.

It follows from (8.5) and that for considered values of the parameter $k \neq 2$, we will have

$$n = A \left[\frac{1}{a_0^{(k-2)/2}} - \frac{1}{a^{(k-2)/2}} \right], \qquad (8.7)$$

where

$$A = \frac{2}{(k-2)C\kappa_0^k}.$$

Unstable crack growth is obtained after $n = n^{\mathrm{cr}}$ cycles when the critical crack length a_{cr} satisfies the limiting relation

$$(K_{\max})_{a=a_{\mathrm{cr}}} = K_{\mathrm{C}}$$

or, in another form, we have

$$\beta \frac{T_{\max}}{h} \sqrt{\pi a_{\mathrm{cr}}} = K_{\mathrm{C}}. \qquad (8.8)$$

The quantities $\sigma_{\max}$ and $T_{\max}$ (respectively $\sigma_{\min}$ and $T_{\min}$) are the maximum (minimum) stresses and tensions in the uncracked plate, where the crack is located. Using (8.8) and the inequality $\Delta T / T_0 \ll 1$, we obtain

$$a_{\mathrm{cr}} = \frac{1}{\pi} \left(\frac{K_{\mathrm{C}} h}{\beta T_{\max}} \right)^2 \approx \frac{1}{\pi} \left(\frac{K_{\mathrm{C}} h}{\beta T_0} \right)^2$$

and, consequently, we will have the following expression for the critical number of cycles:

$$n^{\mathrm{cr}} = (n)_{a=a_{\mathrm{cr}}} = A \left[\frac{1}{a_0^{(k-2)/2}} - \left(\frac{\sqrt{\pi} \beta T_0}{K_{\mathrm{C}} h} \right)^{k-2} \right]. \qquad (8.9)$$

From the condition of positiveness of the expression in (8.9), we find the maximum value of admissible tensions,
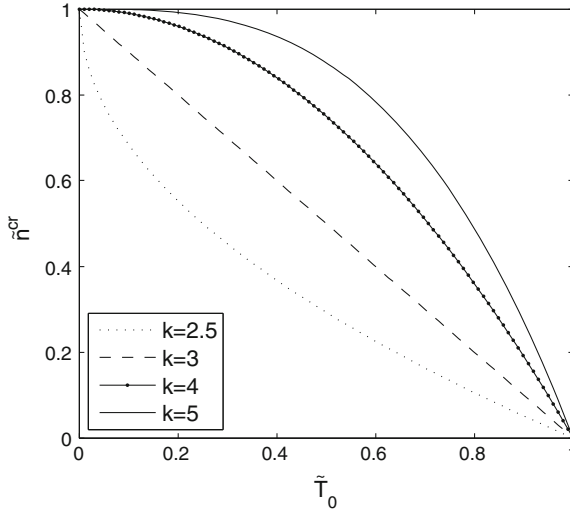
Fig. 8.2 Dependence of the normalized critical number of cycles, (8.25), on the dimensionless average tension, (8.20)

$$T_0 \leq \frac{1}{\sqrt{\pi a_0}} \frac{K_C h}{\beta} \equiv T_0^{\mathrm{M}} . \tag{8.10}$$

In the special case $k = 2$, we can find the critical number of cycles to be

$$n^{\mathrm{cr}} = B \ln\left[\frac{1}{\pi a_0} \left(\frac{K_C h}{\beta T_0} \right)^2 \right] , \tag{8.11}$$

where

$$B = \frac{1}{C \kappa_0^2} ,$$

and the tension limit T_0^{M} is expressed by (8.10).

The dependence of the critical number of cycles n^{cr} on the average tension T_0 and the problem parameter k is shown in Fig. 8.2 using dimensionless quantities that will be presented below in (8.19) and (8.24).

The critical velocity of static instability (buckling) of the travelling plate, as was discussed in Sect. 3.4 (see also Banichuk et al. 2010), is given by the following formula:

$$(V_0^{\mathrm{cr}})^2 = \frac{T_0}{m} + \frac{\gamma_*^2}{m} \frac{\pi^2 D}{\ell^2} , \tag{8.12}$$

where $D = Eh^3 / \left[12 \left(1 - \nu^2 \right) \right]$, m is the mass per unit area (of the plate), and $\gamma = \gamma_*$ is the root of the equation (see Fig. 3.3)

$$\Phi(\gamma, \mu) - \Psi(\gamma, \nu) = 0 , \tag{8.13}$$

where

$$\Phi(\gamma, \mu) = \tanh\left(\frac{\sqrt{1-\gamma}}{\mu}\right) \coth\left(\frac{\sqrt{1+\gamma}}{\mu}\right) ,$$

$$\Psi(\gamma, \nu) = \frac{\sqrt{1+\gamma}}{\sqrt{1-\gamma}} \frac{(\gamma + \nu - 1)^2}{(\gamma - \nu + 1)^2} , \qquad \mu = \frac{\ell}{\pi b} . \tag{8.14}$$

As is seen from (8.13) and (8.14), the root $\gamma = \gamma_*$ depends on ν and μ, and does not depend on the other problem parameters including the value of tension T_0. Consequently, the critical instability velocity, defined in (8.12), increases when tension T_0 is increased. However, T_0 cannot be increased indefinitely due to initial damages and other imperfections.

8.1.2 Finding Optimal Solution

The most important factor, for the runnability and stability of moving plates containing initial imperfections, is the applied tension. To find a safe and optimal T_0 maximizing the performance function is the problem we will consider in this section.

Let us represent the functional to be optimized, (8.4), as a function of the average tension T_0. By taking into account explicit expressions for n^{cr}, in (8.9), and for V_0^{cr}, in (8.12), and performing necessary algebraic transformations, assuming that $k \neq 2$, we will have

$$J(T_0) = m_0 \tau V_0^{\mathrm{cr}}(T_0) n^{\mathrm{cr}}(T_0)$$
$$= J_0 \left[1 + \frac{1}{D}\left(\frac{\ell}{\gamma_* \pi}\right)^2 T_0\right]^{1/2} \left[1 - \left(\frac{\beta \sqrt{\pi a_0}}{h K_C} T_0\right)^{k-2}\right] \tag{8.15}$$

where

$$J_0 = m_0 \tau C_{V_0} C_n , \tag{8.16}$$

and

$$C_{V_0} = \frac{\pi \gamma_* \sqrt{D}}{\ell \sqrt{m}} \tag{8.17}$$

and

$$C_n = \frac{2a_0}{(k-2)C}\left(\frac{h}{2\beta \Delta T \sqrt{\pi a_0}}\right)^k . \tag{8.18}$$

The performance function J is proportional to the multiplier J_0, and consequently, the optimized tension T_0 does not depend on J_0.

For convenience of the following estimations and reduction of characteristic parameters, we introduce the dimensionless values

$$\tilde{J} = \frac{J}{J_0} \, , \tag{8.19}$$

$$\tilde{T}_0 = \frac{T_0}{T_0^{\mathrm{M}}} = \frac{\beta \sqrt{\pi a_0}}{K_C h} T_0 \, , \tag{8.20}$$

$$g = \frac{K_C h}{\beta D \sqrt{\pi a_0}} \left(\frac{\ell}{\gamma_* \pi} \right)^2 \, . \tag{8.21}$$

The optimized functional and the interval of optimization, in the case when $k > 2$, are

$$\tilde{J}(\tilde{T}_0) = \left(1 + g \tilde{T}_0 \right)^{1/2} \left(1 - \tilde{T}_0^{k-2} \right) \, , \tag{8.22}$$

with

$$0 \le \tilde{T}_0 \le 1 \, . \tag{8.23}$$

In other words, we consider

$$\tilde{J}(\tilde{T}_0) = \tilde{V}_0^{\mathrm{cr}}(\tilde{T}_0) \, \tilde{n}^{\mathrm{cr}}(\tilde{T}_0)$$

with

$$\tilde{V}_0^{\mathrm{cr}}(\tilde{T}_0) = \left(1 + g \tilde{T}_0 \right)^{1/2} \tag{8.24}$$

and

$$\tilde{n}^{\mathrm{cr}}(\tilde{T}_0) = 1 - \tilde{T}_0^{k-2} \, . \tag{8.25}$$

In the special case $k = 2$, we will use the expressions (8.4), (8.11) and (8.12), and perform algebraic transformations. We will have

$$J(T_0) = m_0 \tau \, V_0^{\mathrm{cr}}(T_0) n^{\mathrm{cr}}(T_0)$$

$$= J_1 \left[1 + \frac{1}{D} \left(\frac{\ell}{\gamma_* \pi} \right)^2 T_0 \right]^{1/2} \ln \left(\frac{h K_C}{\beta \sqrt{\pi a_0}} \frac{1}{T_0} \right)$$

with

$$J_1 = \frac{2 m_0 \tau \pi \gamma_* \sqrt{D}}{C \ell \sqrt{m}} \left(\frac{h}{2 \beta \Delta T \sqrt{\pi}} \right)^2 \, .$$

Using the dimensionless values $\tilde{J} = J/J_1$ and $\tilde{T}_0$, g from (8.19)–(8.21), we find that

$$\tilde{J}(\tilde{T}_0) = \ln \left(\frac{1}{\tilde{T}_0} \right) \left(1 + g \tilde{T}_0 \right)^{1/2} \, , \qquad 0 \le \tilde{T}_0 \le 1 \, . \tag{8.26}$$

Table 8.1 Physical parameters used in the numerical examples

Material constants				
E	ν	m	G_C/ρ (Seth and Page 1974)	C
10^9 N/m^2	0.3	0.08 kg/m^2	10 Jm/kg	10^{-14}

Geometric constants			
ℓ	$2b$	h	β
0.1 m	10 m	10^{-4} m	1.12

It is seen from (8.26) that

$$0 = (\tilde{J})_{\tilde{T}_0=1} \leq \tilde{J}(\tilde{T}_0) \leq \lim_{\tilde{T}_0 \to 0} (\tilde{J}) = \infty , \qquad 0 \leq \tilde{T}_0 \leq 1 . \qquad (8.27)$$

Note that (8.27) also holds in the case $k < 2$, when

$$\tilde{J}(\tilde{T}_0) = - \left(1 + g\tilde{T}_0\right)^{1/2} \left(1 - \tilde{T}_0^{k-2}\right)$$

and

$$J_0 = \frac{2m_0\tau\pi a_0\gamma_* \sqrt{D}}{(2-k)C\ell\sqrt{m}} \left(\frac{h}{2\beta\Delta T \sqrt{\pi a_0}}\right)^k .$$

Thus, in the case $k \leq 2$, the optimum is $\tilde{T}_0 = 0$, which is not a physically meaningful case, since it corresponds to an extremely low plate velocity. However, for most materials $k \approx 3$ or bigger.

8.1.3 Dependence of Optimal Solution on Problem Parameters

In the following, we will look at some numerical examples. The optimization problem (8.22)–(8.23) is solved numerically for different values of k: for $k = 2.5$, $k = 3$ and $k = 3.5$. The material parameters are chosen to describe a paper material. The parameter values used in the examples are given in Table 8.1. Paper fracture toughness K_C is calculated from the fundamental relation $G_C = K_C^2/E$. The variance in tension is chosen to be small, $\Delta T = 0.1$ N/m. The values of initial crack lengths used in the examples are $a_0 = 0.005, 0.01, 0.05, 0.1$ m. As illustrated in Fig. 8.1, the length of one cycle is assumed to be 2ℓ. This value is used to approximate the cycle time period τ by $\tau = 2\ell/V_0^{cr}$ after the value of V_0^{cr} is evaluated by the optimization.

In Fig. 8.3, the dimensionless performance function (8.22) is plotted for $k = 2.5, 3, 3.5$. It is seen that the value of optimal tension $\tilde{T}_0^*$ is increased with increasing k.

In Tables 8.2 and 8.3, the results of the nondimensional optimization problem (8.22)–(8.23) are shown for the considered values of parameters k and a_0. In Table 8.2, the values of the productivity function $\tilde{J}$ at the optimum are shown.
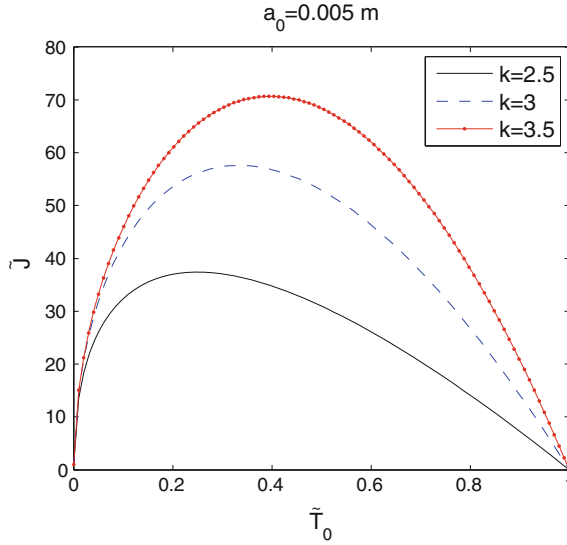
Fig. 8.3 Performance dependence on tension (dimensionless quantities). The dimensionless parameters and functions are presented in (8.19)–(8.22)

Table 8.2 Dependence of the optimum of the performance $\tilde{J}$ on the Paris material constant k and the initial crack length a_0

$\tilde{J}^*$	a_0 (m)			
	0.005	0.01	0.05	0.1
$k = 2.5$	37.4023	31.4527	21.0369	17.6920
$k = 3$	57.5834	48.4230	32.3862	27.2358
$k = 3.5$	70.6836	59.4390	39.7532	33.4308

An increase in the length of the initial crack a_0 is seen to decrease productivity. The values of productivity seem to increase when k is increased. However, one must take into account that also J_0, in (8.16)–(8.17), depends on k, which affects the actual productivity $J = J_0 \tilde{J}$.

In Table 8.3, the optimal values of the dimensionless tension $\tilde{T}_0^*$ are shown. It is seen that the optimal dimensionless tension values slightly decrease when the crack length is increased.

Since the actual optimal productivity, the actual tension, and the related critical speed and the critical number of cycles are of interest, these values were found at the optimum and are shown in Tables 8.4 and 8.5.

Note that several assumptions have been made. First, the Paris constant $C = 10^{-14}$ is assumed to be independent of k, and both of the values are not measured for paper, but were chosen to be close to the typical values of some known materials. Secondly, the cycle time period τ is approximated assuming that one cycle length is 2ℓ, that is, $\tau = 2\ell/V_0^{\text{cr}}$.

Table 8.3 Dependence of optimal dimensionless tension $\tilde{T}_0^*$ on the Paris material constant k and the initial crack length a_0

$\tilde{T}_0^*$	a_0 (m)			
	0.005	0.01	0.05	0.1
$k = 2.5$	0.2500	0.2499	0.2499	0.2498
$k = 3$	0.3333	0.3333	0.3332	0.3332
$k = 3.5$	0.3968	0.3968	0.3968	0.3967

Table 8.4 *Top* Dependence of the optimal tension T_0^* (N/m) on the Paris material constant k and the initial crack length a_0 (m). *Bottom* Critical velocity V_0^{cr} (m/s) at the optimum, depending on the parameters k and a_0

T_0^* (N/m)	a_0 (m)			
	0.005	0.01	0.05	0.1
$k = 2.5$	504	356	159	113
$k = 3$	672	475	212	150
$k = 3.5$	800	565	253	179
$V_0^{cr}(T_0^*)$ (m/s)	a_0 (m)			
	0.005	0.01	0.05	0.1
$k = 2.5$	79.352	66.727	44.623	37.523
$k = 3$	91.628	77.051	51.529	43.332
$k = 3.5$	99.979	84.073	56.226	47.282

The actual optimal tension T_0^* is calculated from (8.19), that is $T_0^* = T_0^M \tilde{T}_0^*$. Since T_0^M depends only on fixed values, and the material parameters in T_0^M are measured and known for paper materials, the results for the actual optimal tension, shown in Table 8.4, left, are comparable and quite reliable. The results for the optimal tension T_0^* are also illustrated as a colorsheet in Fig. 8.4.

In Table 8.4, right, the critical velocities corresponding to the optimal values of tension $V_0^{cr}(T_0^*)$ are shown. The values of velocities can be calculated directly from (8.12) using the values in Table 8.4a. As expected, the velocities decrease as a_0 is increased.

The actual optimal number of cycles $n^{cr}(T_0^*)$ and the actual optimal productivity J^* are more difficult to predict, since they depend on the Paris constant C, which is not known for paper materials. As mentioned above, the same value of C, namely $C = 10^{-14}$, is used for all investigated values of k, which might not be reasonable. Since the value of κ_0 defined in (8.5) is large (the numerical value of κ_0 is larger than unity), then κ_0^k increases with the increase in k. Keeping C constant, we see from (8.5) that the crack growth rate may be larger for a large value of k, depending on the value of $a^{k/2}$, which is small. This means that the number of cycles may be the smaller the greater the value of k is, which can also be seen from (6.11): the greater the value of k, the smaller the value of A. In the results in Table 8.5, top, it can be seen that the effect of κ_0 is large, and the number of cycles at the optimum decreases remarkably when k is increased. This also results in a decrease in the optimal productivity J^*, which is shown in Table 8.5, bottom.
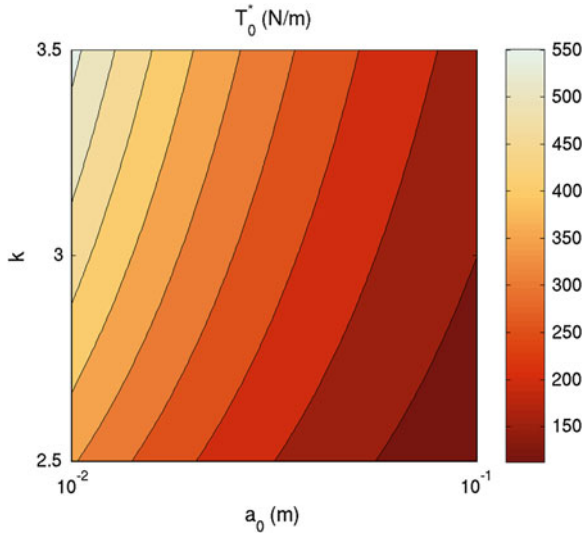
Fig. 8.4 A colorsheet showing the dependence of the optimal tension T_0^* (N/m) on the parameters k (Paris material constant) and a_0 (initial crack length). Note the logarithmic scale of a_0

Table 8.5 *Top* The number of cycles n^{cr} at the optimum, depending on the parameters k and a_0. *Bottom* Dependence of the optimum of the performance J (kg) on the Paris material constant k and the initial crack length a_0 (m)

$n^{\text{cr}}(T_0^*)$	a_0 (m)			
	0.005	0.01	0.05	0.1
$k = 2.5$	757,300	636,834	425,943	358,216
$k = 3$	30,130	21,306	9,529	6,738
$k = 3.5$	1,348	801	239	142
J^* (kg)	a_0 (m)			
	0.005	0.01	0.05	0.1
$k = 2.5$	121,168	101,894	68,151	57,315
$k = 3$	4,821	3,409	1,525	1,078
$k = 3.5$	216	128	38	23

Comparing the results in Tables 8.2 and 8.5, top, we therefore make no conclusion about the effect of k on the actual performance J^*. The qualitative result of the decrease in performance J^* when a_0 is increased is, however, plausible.

8.2 Pareto Optimal Solutions for Good Runnability

In this section, we seek an optimal in-plane tension that maximizes a performance vector function consisting of the critical velocity, the number of cycles before fracture and process effectiveness. The considered problem of multiple objectives is called

a multi-objective optimization (multi-objective programming or multi-criteria optimization) problem. Necessary conditions for the optimality of the maximized vector function are derived, and the Pareto optimal solutions are found analytically for some example cases.

As was seen above, optimal magnitude of tension is essential for safe conditions in systems with axially travelling material. Seeking the optimal tension but having several objectives, such as high material longevity, transport velocity and productivity, we encounter a multi-objective optimization problem. Extensive literature reviews on multi-objective optimization are provided by White (1990) and Miettinen (1994). For a historical review of the origin and development of multicriteria optimization, refer to Stadler (1979). For surveys of concepts and methods of multi-objective optimization, see Chankong and Haimes (1983) and Steuer (1986).

Below, we will derive the multiobjective optimization problem consisting of maximizing the critical plate velocity, the longevity (critical number of loading cycles) and the productivity with respect to the value of in-plane tension. We concentrate especially on paper making productivity, though the analysis is also applicable to any other analogous processes.

The obtained objective vector function is transformed into a scalar objective function using the weighting method. For several important subproblems, the optimal value of tension is found analytically in the Pareto sense with respect to the other problem parameters.

8.2.1 Multicriteria Optimization

We consider again an axially moving elastic plate which is travelling between a system of rollers. See Fig. 8.1.

All the plate elements

$$\Omega_i \equiv \left\{ (x, y) \in \mathbb{R}^2 \mid i\ell < x < (i + 1)\ell, \ -b < y < b \right\}, \quad i = 0, 1, 2, \dots$$

are subjected to homogeneous (in the y direction) tension T acting in the x direction. The sides

$$\{ x = i\ell, \ -b \le y \le b \} \quad \text{and} \quad \{ x = (i + 1)\ell, \ -b \le y \le b \}$$

are simply supported and the sides

$$\{ y = -b, \ i\ell \le x \le (i + 1)\ell \} \quad \text{and} \quad \{ y = b, \ i\ell \le x \le (i + 1)\ell \}$$

are free of tractions.

We present a productivity criterion (performance function) with the help of the plate velocity V_0 and the process time t_f:

$$M = m_0 V_0 t_{\mathrm{f}} \ , \qquad m_0 = 2bm \ . \tag{8.28}$$

In (8.28), the velocity V_0 is taken from the safe interval

$$0 < V_0 < V_0^{\mathrm{cr}} \ ,$$

where V_0^{cr} is the critical buckling velocity that is also taken as a criterion of the considered process:

$$J_{\mathrm{V}} \equiv V_0^{\mathrm{cr}} \ , \tag{8.29}$$

where V_0^{cr} is expressed by (8.12).

A safe interval for the safe functioning time (number of cycles) is written as

$$0 < t_{\mathrm{f}} < t_{\mathrm{f}}^{\mathrm{cr}} \quad \text{or} \quad 0 < n < n^{\mathrm{cr}} \ ,$$

where $t_{\mathrm{f}}^{\mathrm{cr}}$ and n^{cr} are, respectively, the time interval and the total number of cycles before fatigue fracture.

For a small cycle time period τ and a big number of cycles n, we assume that $t_{\mathrm{f}} \approx n\tau$.

We will consider the critical number of cycles as a safety function J_{N}, i.e.,

$$J_{\mathrm{N}} \equiv n^{\mathrm{cr}} \ , \tag{8.30}$$

where n^{cr} is given by (8.9), or (8.11) in the case of $k = 2$. The productivity criterion M^{cr} is also considered as a problem function

$$J_{\mathrm{M}} \equiv M^{\mathrm{cr}} \ , \tag{8.31}$$

where M^{cr} is given by (8.28) with critical parameter values. We have

$$J_{\mathrm{M}} = m_0 J_{\mathrm{V}} t_{\mathrm{f}}^{\mathrm{cr}} = m_0 \tau J_{\mathrm{V}} J_{\mathrm{N}} \ . \tag{8.32}$$

Note that the functions J_{V}, J_{N} and J_{M} defined in (8.29), (8.30) and (8.31) depend on the value of in-plane average tension T_0:

$$J_{\mathrm{V}} = J_{\mathrm{V}}(T_0) \ ,$$
$$J_{\mathrm{N}} = J_{\mathrm{N}}(T_0) \ ,$$
$$J_{\mathrm{M}} = J_{\mathrm{M}}(T_0) \ .$$

Using the limit velocity V_0, longevity n and runnability effectiveness M criteria, presented in the previous section, we may consider the following vector function

$$J = \left\{ \begin{array}{c} J_V(T_0) \\ J_N(T_0) \\ J_M(T_0) \end{array} \right\} = \left\{ \begin{array}{c} V_0^{\mathrm{cr}}(T_0) \\ n^{\mathrm{cr}}(T_0) \\ M^{\mathrm{cr}}(T_0) \end{array} \right\} . \tag{8.33}$$

Now, we formulate the multicriteria (multiobjective) optimization problem. It is required to determine the optimal value T_0^* of in-plane tension T_0 that gives a maximum of the considered vector function, i.e.

$$J^* = J(T_0^*) = \max_{T_0} \; J(T_0) . \tag{8.34}$$

The values in (8.33) and (8.34) are determined with the help of the corresponding formulas and relations presented in Sects. 8.1.1 and 8.1.2.

The max operation in (8.34) is considered in the Pareto sense. It is:

$$T_0^* = \arg \max_{T_0} \; J(T_0)$$

if there is no other value $\hat{T}_0$, such that

$$J_i(\hat{T}_0) \geq J_i(T_0^*), \quad i = \mathrm{V}, \mathrm{N}, \mathrm{M} ,$$

and the following rigorous inequality is satisfied for at least one component criterion:

$$J_j(\hat{T}_0) > J_j(T_0^*) .$$

To solve this multiobjective optimization problem, we apply the weighting method. We formulate the preference function as a sum of the single objective functionals J_V, J_N, J_M associated with the weighting factors C_V, C_N, C_M:

$$J_C = C_V J_V + C_N J_N + C_M J_M , \tag{8.35}$$

and we suppose that

$$C_V \geq 0, \quad C_N \geq 0, \quad C_M \geq 0 ,$$
$$C_V + C_N + C_M = 1 .$$

We will consider the multiobjective optimization problem of finding the optimal in-plane tension T_0^* separately for different particular cases.

For convenience of performing the analysis and for reduction of characteristic parameters, we introduce the following values with tildes

$$\tilde{J}_V = \frac{J_V}{J_V^0} , \qquad\qquad J_V^0 = \sqrt{\frac{K_C h}{m \beta \sqrt{\pi a_0}}} ,$$

$$\tilde{J}_{\mathrm{N}} = \frac{J_{\mathrm{N}}}{J_{\mathrm{N}}^0} \,, \qquad\qquad J_{\mathrm{N}}^0 = \frac{2}{(k-2)C\kappa_0^k a_0^{(k-2)/2}} \,, \qquad (8.36)$$

$$\tilde{J}_{\mathrm{M}} = \frac{J_{\mathrm{M}}}{J_{\mathrm{M}}^0} \,, \qquad\qquad J_{\mathrm{M}}^0 = m_0 \tau J_{\mathrm{V}}^0 J_{\mathrm{N}}^0 \,,$$

and represent the criterion functions as

$$\begin{aligned}
\tilde{J}_{\mathrm{V}} &= \left(\tilde{T}_0 + d\right)^{1/2} \,, \\
\tilde{J}_{\mathrm{N}} &= 1 - \tilde{T}_0^{\,k-2} \,, \\
\tilde{J}_{\mathrm{M}} &= \tilde{J}_{\mathrm{V}} \tilde{J}_{\mathrm{N}} \,,
\end{aligned} \qquad (8.37)$$

using the dimensionless values and problem parameters:

$$\tilde{T}_0 = \frac{\beta \sqrt{\pi a_0}}{K_{\mathrm{C}} h} T_0 \,, \qquad d = \frac{\gamma_*^2 \pi^2 D\beta \sqrt{\pi a_0}}{l^2 K_{\mathrm{C}} h} \,, \qquad 0 \le \tilde{T}_0 \le 1 \,. \qquad (8.38)$$

8.2.2 Maximizing Critical Velocity and Safety Criterion

We consider the case of maximization of the velocity criterion $\tilde{J}_{\mathrm{V}}$ and the safety criterion $\tilde{J}_{\mathrm{N}}$ when $k = 3$. In this case, we have

$$\begin{aligned}
\tilde{J}_1 &\equiv C_{\mathrm{V}} \tilde{J}_{\mathrm{V}} + C_{\mathrm{N}} \tilde{J}_{\mathrm{N}} \,, \\
C_{\mathrm{V}} + C_{\mathrm{N}} &= 1 \,.
\end{aligned} \qquad (8.39)$$

Let us study the solution of (8.39) with respect to the weight C_{N}. Now, the optimization problem is (note $C_{\mathrm{V}} = 1 - C_{\mathrm{N}}$)

$$\max_{0 \le \tilde{T}_0 \le 1} (1 - C_{\mathrm{N}})(\tilde{T}_0 + d)^{1/2} + C_{\mathrm{N}}(1 - \tilde{T}_0) \,. \qquad (8.40)$$

The object function in (8.40) is concave, so the use of the weighting method is justifiable for finding the Pareto optimal solutions.

Depending on the value of the weight C_{N}, the optimal value of the dimensionless tension $\tilde{T}_0^*$, which in this case can be found at the at the zero of the derivative of the objective function $\tilde{J}_1$, is

$$0 \le C_{\mathrm{N}} \le \frac{1}{1 + 2\sqrt{d+1}} : \qquad \tilde{T}_0^* = 1 \,,$$

$$\frac{1}{1 + 2\sqrt{d+1}} < C_{\mathrm{N}} < \frac{1}{1 + 2\sqrt{d}} : \qquad \tilde{T}_0^* = \left(\frac{1 - C_{\mathrm{N}}}{2C_{\mathrm{N}}}\right)^2 - d \,,$$

Fig. 8.5 The Pareto front (PF) for the problem of maximizing the critical velocity $\tilde{J}_V$ and safety criterion $\tilde{J}_N$. See (8.37) and (8.41). A schematic figure
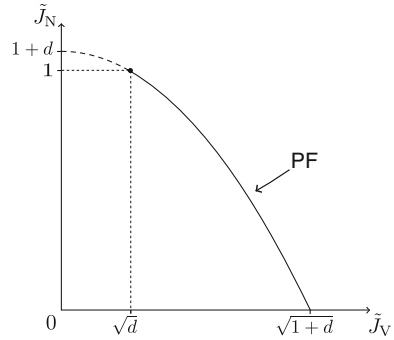
$$\frac{1}{1+2\sqrt{d}} \leq C_N \leq 1 : \qquad\qquad \tilde{T}_0^* = 0 .$$

Consequently, the values of the component functions are found in the following form:

$$\tilde{J}_V = \sqrt{\tilde{T}_0^* + d} = \frac{1 - C_N}{2C_N} ,$$

$$\tilde{J}_N = 1 - \tilde{T}_0^* = 1 + d - \left(\frac{1 - C_N}{2C_N}\right)^2 ,$$

and, for the considered problem of critical velocity and longevity maximization, the Pareto front (PF) of the optimal solution is given by the equation

$$\tilde{J}_N = 1 + d - \tilde{J}_V^2 , \tag{8.41}$$

where

$$\tilde{J}_V \in [\sqrt{d}, \sqrt{1+d}] .$$

The Pareto front is represented in Fig. 8.5.

8.2.3 Maximizing Critical Velocity and Process Effectiveness

Consider now another case, where we maximize the critical velocity criterion $\tilde{J}_V$ and the process effectiveness criterion $\tilde{J}_M$. We discuss again the case with $k = 3$. In this case, the weighting method problem is

$$\tilde{J}_2 \equiv C_V \tilde{J}_V + C_M \tilde{J}_M ,$$

$$C_V + C_M = 1 ,$$

so that we study

$$\max_{0 \le \tilde{T}_0 \le 1} \left[C_V (\tilde{T}_0 + d)^{1/2} + C_M (\tilde{T}_0 + d)^{1/2} (1 - \tilde{T}_0) \right] . \tag{8.42}$$

The object function in (8.42) is concave. Now, the extremum condition is

$$\begin{aligned}
\frac{d\tilde{J}_2}{d\tilde{T}_0} &= C_V \frac{d\tilde{J}_V}{d\tilde{T}_0} + C_M \frac{d\tilde{J}_M}{d\tilde{T}_0} \\
&= C_V \frac{d\tilde{J}_V}{d\tilde{T}_0} + C_M \left(\tilde{J}_N \frac{d\tilde{J}_V}{d\tilde{T}_0} + \tilde{J}_V \frac{d\tilde{J}_N}{d\tilde{T}_0} \right) \\
&= 0 .
\end{aligned} \tag{8.43}$$

The solution of the problem is studied with respect to the weight C_M (note again $C_V = 1 - C_M$). By (8.43), it is found that the optimal value for the dimensionless tension $\tilde{T}_0^*$ depends on C_M as follows:

$$0 \le C_M \le \frac{1}{2d+3} : \qquad \tilde{T}_0^* = 1$$

$$\frac{1}{2d+3} < C_M \le 1 : \qquad \tilde{T}_0^* = \frac{1 - 2dC_M}{3C_M} .$$

For the optimized functionals $\tilde{J}_V$ and $\tilde{J}_M$, we have

$$\tilde{J}_V^2 = \frac{1}{3} \left(\frac{1}{C_M} + d \right) ,$$

$$\tilde{J}_M = \frac{1}{3} \left(2d + 3 - \frac{1}{C_M} \right) \sqrt{\frac{1}{3} \left(\frac{1}{C_M} + d \right)} .$$

The Pareto front of the problem under consideration is described by the equation

$$\tilde{J}_M = (1 + d)\tilde{J}_V - \tilde{J}_V^3 \tag{8.44}$$

defined on the interval

$$\tilde{J}_V \in \left[\sqrt{(1+d)/3}, \sqrt{1+d} \right]$$

and is shown in Fig. 8.6.
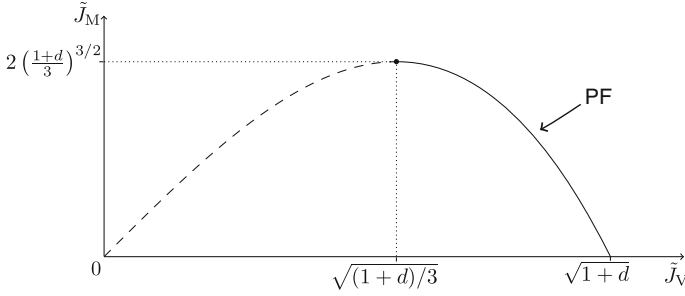
Fig. 8.6 The Pareto front (PF) for the problem of maximizing the critical velocity $\tilde{J}_V$ and the criterion of process effectiveness $\tilde{J}_M$. See (8.37) and (8.44). A schematic figure

8.2.4 Maximizing Safety and Process Effectiveness

As a third case, we study the maximization of the safety criterion $\tilde{J}_N$ and the process effectiveness criterion $\tilde{J}_M$ when $k = 3$. We have

$$\tilde{J}_3 \equiv C_N \tilde{J}_N + C_M \tilde{J}_M ,$$

$$C_N + C_M = 1 ,$$

and the optimization problem reads

$$\max_{0 \leq \tilde{T}_0 \leq 1} \left[C_N(1 - \tilde{T}_0) + (1 - C_N)(\tilde{T}_0 + d)^{1/2}(1 - \tilde{T}_0) \right] . \tag{8.45}$$

Also the object function $\tilde{J}_3$ is concave. We study the problem (8.45) with respect to the weight C_N. Now the optimal value of the dimensionless tension $\tilde{T}_0^*$ depends on C_N in the following way:

$$0 \leq C_N < \frac{1 - 2d}{1 - 2d + 2\sqrt{d}} : \qquad \tilde{T}_0^* = \frac{2}{9}\Big(\alpha^2 - 3d + 3/2$$
$$- \alpha\sqrt{\alpha^2 + 3d + 3}\Big) ,$$

$$\frac{1 - 2d}{1 - 2d + 2\sqrt{d}} \leq C_N \leq 1 : \qquad \tilde{T}_0^* = 0 ,$$

where

$$\alpha \equiv \frac{C_N}{C_M} = \frac{C_N}{1 - C_N} . \tag{8.46}$$
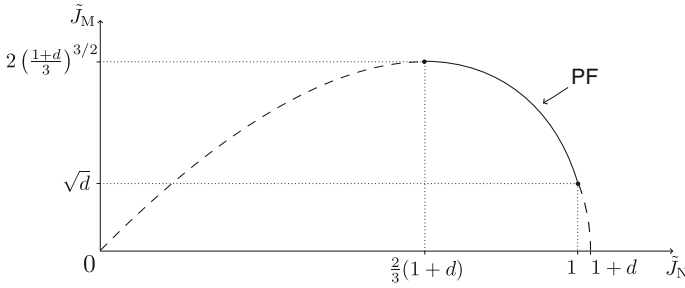
Fig. 8.7 The Pareto front (PF) for the problem of maximizing the critical number of cycles $\tilde{J}_N$ and the criterion of process effectiveness $\tilde{J}_M$. See (8.37) and (8.47). A schematic figure

In this case, the Pareto front is given by

$$\tilde{J}_M = \tilde{J}_N\sqrt{1 + d - \tilde{J}_N}\ , \qquad \tilde{J}_N \in \left[\frac{2}{3}(1 + d), 1\right] . \qquad (8.47)$$

See Fig. 8.7.

Finally, note that the maximum of (8.35) in the case $C_M = 1$ and $C_V = C_N = 0$ is found above by solving the problems (8.42) and (8.45). Then,

$$\tilde{J}_V = \sqrt{(1 + d)/3} \quad \text{and} \quad \tilde{J}_N = \frac{2}{3}(1 + d) ,$$

which is also a Pareto optimal solution for the problem (8.40) confirmed by (8.41).

8.2.5 Some Illustrations

In the previous section, the multi-objective optimization problems of maximizing the critical velocity, maximizing the longevity and maximizing the process effectiveness were studied, and analytical results were found for some special subproblems.

The obtained analytical results are illustrated numerically in this section. Parameter values (material and geometrical) are given in Table 8.6. The paper fracture toughness is $K_C = \sqrt{G_C E}$. The investigated critical crack length a_0 obtains the values 0.005, 0.01, 0.05 and 0.1 m.

The Pareto fronts (8.41), (8.44) and (8.47) are illustrated in Fig. 8.8 when the initial crack length is $a_0 = 0.01$ m.

In Fig. 8.9, the optimal values of tension T_0^* (N/m) for the problems (8.40), (8.42) and (8.45) are plotted with respect to the weights (C_N, C_M and C_N, respectively) and the initial length of the crack a_0.

In Fig. 8.9, top, we present the optimal values of tension T_0^* when the velocity J_V and the longevity J_N are optimized. One may note that the even for a small crack size ($a_0 = 0.01$), the optimal value of tension is almost zero, when the longevity is

Table 8.6 Physical parameters used in the numerical examples

Material constants			
E	ν	m	G_C/ρ (Seth and Page 1974)
10^9 N/m^2	0.3	0.08 kg/m^2	10 Jm/kg
Geometric constants			
ℓ	$2b$	h	β
0.1 m	10 m	10^{-4} m	1.12

given a large weight ($C_N > 0.8$). Weighting the velocity, the optimal tension obtains very large values ($T_0^* \sim 1400$ N/m). In other words, changing the weights radically changes the optimal result. In this case, it is difficult to decide how to weight the object functions.

In Fig. 8.9, middle, we weight the velocity function J_V against the process effectiveness function J_M. In this case, it is noted that the length of the initial crack length significantly affects the optimal value of tension.

Figure 8.9, bottom, shows the third case, where the longevity J_N and the process effectiveness J_M are compared. Also here, it is seen that a_0 has an effect on the value of optimal tension, especially when the process effectiveness is weighted.

Note that the case $C_M = 1$ and $C_V = C_N = 0$ is included in both middle and bottom parts of Fig. 8.9, giving the lowest values for tension in the middle figure and the highest values in the bottom figure. Analyzing these two subproblems helps us to make decisions on the weights to be selected. The optimum for process effectiveness gives some kind of reference value for the desired tension.

With the help of Fig. 8.9, we have chosen some values for the weights C_N and C_M. The solutions are collected into Table 8.7.

8.3 Optimization with Uncertainties

In this section, we present a stochastic analysis of axially moving cracked elastic plates with uncertainties. The study is focused on instability and material fracture, which are the most serious threats to stable production of a papermachine. On these phenomena a change in tension magnitude has opposite effects. Increasing the magnitude of tension has a stabilizing effect but it may lead to growing of cracks. We will present an analysis to find the optimal value of velocity and tension for efficient product processing.

In last decades, the studies of runnability have been based on a deterministic approach. However, we know that in practice the values of different parameters are not known precisely and the process to be modelled usually includes random factors. At the last section of this book, we would like to raise awareness of this and offer one relatively simple approach to consider this issue.

Fig. 8.8 Pareto fronts for
the problems $\max\{\tilde{J}_N, \tilde{J}_V\}$,
$\max\{\tilde{J}_M, \tilde{J}_V\}$, and
$\max\{\tilde{J}_M, \tilde{J}_N\}$, respectively,
in the case when the initial
crack length $a_0 = 0.01$ m
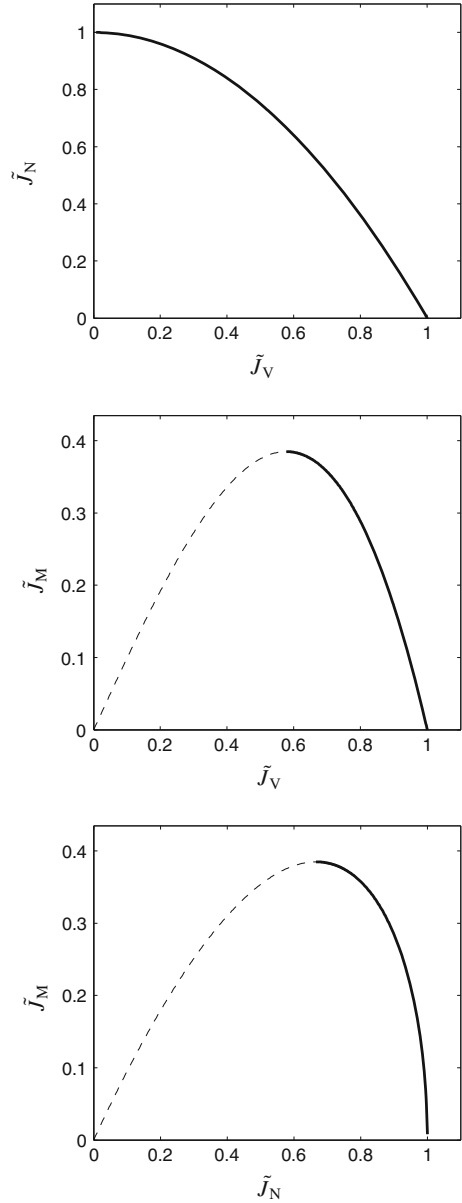
From the application point of view, uncertainty occurs as, e.g., variation of tension, in space and time, in the press system of a papermachine, and defects on a paper web, which vary in their location, size, shape and orientation (Björklund and Svedjebrant 2009; Niskanen 2012). Another example is given by strength of paper which was found to obey the Weibull and Duxbury distributions by Salminen (2003). Accord-

Fig. 8.9 Dependence of
the optimal tension T_0 on
the initial crack length a_0
and the weight C_N or C_M.
(Reproduced from Banichuk
et al. 2013)
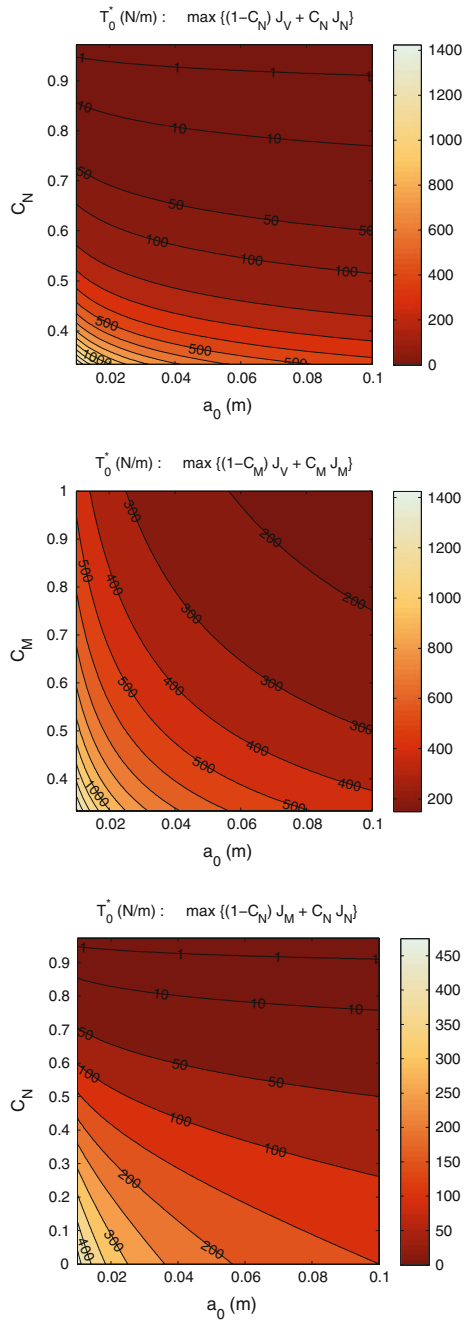
Table 8.7 Dependence of the optimal tension (dimensionless $\tilde{T}_0^*$ and dimensional T_0^*) on the selected weights for the three studied cases. The used initial crack length was $a_0 = 0.01$ m (Banichuk et al. 2013)

arg max$\{C_N J_N + C_V J_V\}$			arg max$\{C_M J_M + C_V J_V\}$		
C_N	$\tilde{T}_0^*$	T_0^* (N/m)	C_M	$\tilde{T}_0^*$	T_0^* (N/m)
0.4	0.5624	801	0.4	0.8333	1,187
0.5	0.2499	356	0.5	0.6666	950
0.6	0.1110	158	0.6	0.5555	791
0.7	0.0459	65	0.7	0.4761	678
0.8	0.0156	22	0.8	0.4166	594
0.9	0.0030	4	0.9	0.3703	528
			1.0	0.3333	475

arg max$\{C_N J_N + C_M J_M\}$		
C_N	$\tilde{T}_0^*$	T_0^* (N/m)
0.0	0.3333	475
0.1	0.2932	418
0.2	0.2500	356
0.3	0.2042	291
0.4	0.1571	224
0.5	0.1111	158
0.6	0.0695	99
0.7	0.0364	52
0.8	0.0143	20
0.9	0.0030	4

ing to Uesaka (2004), the majority of web breaks in paper production are caused by tension variations, combined with strength variations of the paper web. Wathén (2003) discusses the effect of flaws of paper on web breaks and notes that even a seemingly perfect paper can fail at very low tensions due to stress concentrations caused by discontinuities, e.g., cuts and shives, inside the structure. Because of the stochastic structure of paper, it is difficult to predict occurences of flaws. Therefore we include uncertainty aspects in the model and study the problem of finding the optimal velocity from a probabilistic point of view.

There occur a large variety of defects in a paper web during its manufacturing process, but we concentrate on studying a plate with an initial crack at the edge, which can be considered the most usual case. Björklund and Svedjebrant (2009) have found that there is a higher density of defects at the edges of the paper, possibly as a result of greater variance of the steam box control at the edges. Smith (1995) classifies edge cracks as edge cuts or nicks that usually extend only a short distance. A fiber cut in the web or plate is defined as a typically short and straight cut that is located randomly, and is usually at an approximately right angle at the edge. Smith also lists several possible reasons for an occurrence of a broken edge, the list including dry edges, high sheet caliper at the edge, and web overlapping. A fiber cut is caused

when a pulp fiber or shive that is less compactible than the rest of the web, passes through a high pressure nip.

In the following, the theoretical treatment is divided into two parts. In the first part, we assume the moving plate to have an initial crack of random length at the edge, and we formulate analytical expressions for the optimal tension and velocity of the plate. In the second study, the magnitude of homogeneous in-plane tension affecting the plate in the machine direction is assumed to be a random variable, and we derive a formula for the optimal velocity. In this part, the length of the crack is assumed to be constant.

The obtained analytical expressions are used for computing the optimal tension and the corresponding optimal velocity numerically. To do this, we use the log-normal distribution for the crack length and the in-plane tension is modelled with truncated normal distribution. The effect of changing the values of distribution parameters is illustrated. In the case of random crack length we will see that the optimal values decrease when the expected value and variance of the crack length increase. In the case of random tension, it is seen that the more the magnitude of tension is dispersed, the lower is the optimal tension. We will also illustrate the effect of changing the value of the admissible probabilites in the constraints. It will be seen that the optimal values increase when the probabilities increase.

8.3.1 Uncertainty in Initial Crack Length

We consider a rectangular elastic plate, which is supported by rollers at both ends and is moving at a constant velocity V_0. Denotation of this domain is the same as in the previous chapters of this book,

$$\Omega \equiv \left\{ (x, y) \in \mathbb{R}^2 \mid 0 < x < \ell, \ -b < y < b \right\}, \tag{8.48}$$

where ℓ and b are prescribed parameters of length and width. The considered domain Ω is a representation of a thin isotropic elastic plate having constant thickness h, Poisson ratio ν, Young modulus E, and bending rigidity $D = Eh^3 / \left[12 \left(1 - \nu^2 \right) \right]$. The mass of the plate per unit area is denoted by m. We assume that the plate is subjected to homogeneous tension T_0 acting in the x direction. We also assume that the plate travels in the x direction as usual. The supporting rollers are located at both ends of the plate, the other edges are free of traction. Schematic setup of the problem is presented in Fig. 8.10.

Suppose there is an initial crack of mode I (see Fig. 8.11) at the edge of the plate, and let ξ be a positive valued random variable that describes the length of the crack. We consider the stress intensity factor (SIF) related to the crack and want to avoid the stress intensity factor reaching its critical value, known as the critical fracture toughness, at which the crack begins to propagate.

We formulate an optimization problem using a similar approach as is presented in the book by Banichuk and Neittaanmäki (2010). We seek the maximal magnitude
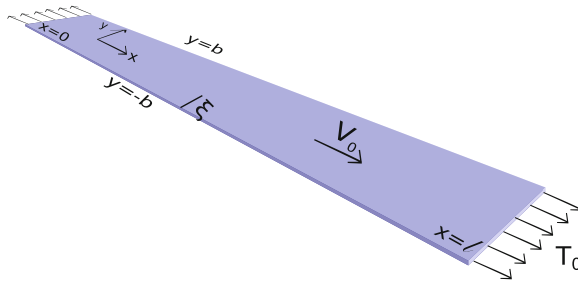
Fig. 8.10 A travelling elastic plate with a crack at the edge

Fig. 8.11 Mode I crack
(opening)
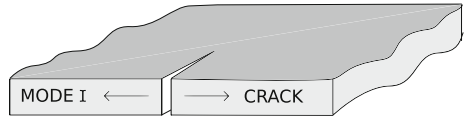
of velocity under the constraint that the probability of fracture is small. Letting $p \in (0, 1)$ denote the probability of fracture that can be accepted, our optimization problem reads as

$$\max_{T_0} V_0^{\mathrm{cr}}(T_0) , \quad \text{such that} \tag{8.49}$$

$$P(K_{\mathrm{I}} \geq K_{\mathrm{IC}}) \leq p , \tag{8.50}$$

where V_0^{cr}, given by (8.12), is the critical velocity, and K_{IC} is the critical fracture toughness of the considered material.

For the stress intensity factor we use the expression

$$K_{\mathrm{I}} = \frac{\alpha(\xi) \, T_0 \sqrt{\pi \xi}}{h} , \tag{8.51}$$

where α is a weight function that depends on the geometry of the domain, the ratio of ξ and b and the ratio of ℓ and b. The formula of α is given, e.g., in Perez (2004), Laham (1998) and Fett (1999). We assume α to be an increasing positive function of ξ and, for simplicity, approximate it as a constant function $\alpha = 1.12$ in this study.

To solve problem (8.49)–(8.50) we are looking for the maximal value of the tension T_0 that satisfies the inequality (8.50) and the equation of stress intensity factor (8.51). The constraint (8.50) is equal to

$$P\left(\xi \geq g^{-1}\left(\frac{K_{\mathrm{IC}} h}{T_0 \sqrt{\pi}}\right)\right) \leq p , \tag{8.52}$$

where g^{-1} is the inverse function of the function $g(\xi) \equiv \alpha(\xi)\sqrt{\xi}$. The inverse function exists, since g is strictly increasing due to the assumptions of α. Further, the inequality above is equal to

$$F_\xi\left(g^{-1}\left(\frac{K_C h}{T_0\sqrt{\pi}}\right)\right) \geq 1 - p \,, \tag{8.53}$$

where F_ξ the cumulative distribution function of ξ. Assuming that ξ has a continuous density function, the function F_ξ is strictly increasing.

Denote

$$\xi_C = F_\xi^{-1}(1 - p) \,. \tag{8.54}$$

The value ξ_C is the minimum of the set

$$\{x : F_\xi(x) \geq 1 - p\} \,. \tag{8.55}$$

Consider another value of crack length $\xi_C^* > \xi_C$. For the values of tension T_C and T_C^* that satisfy

$$\xi_C = g^{-1}\left(\frac{h K_{\mathrm{IC}}}{T_C\sqrt{\pi}}\right) \quad\text{and}\quad \xi_C^* = g^{-1}\left(\frac{h K_{\mathrm{IC}}}{T_C^*\sqrt{\pi}}\right), \tag{8.56}$$

it holds

$$T_C > T_C^* \,. \tag{8.57}$$

Thus, the maximal value of T_0 satisfying (8.50) is found by the equation

$$P(K_{\mathrm{I}} \geq K_{\mathrm{IC}}) = p \,, \tag{8.58}$$

and can be expressed as

$$T^{\mathrm{max}} = \frac{h K_{\mathrm{IC}}}{\alpha(F_\xi^{-1}(1 - p))\sqrt{\pi F_\xi^{-1}(1 - p)}} \,, \tag{8.59}$$

The solution of the optimization problem (8.49)–(8.50) is

$$(V_0)_{\mathrm{opt}} = V_0^{\mathrm{cr}}(T^{\mathrm{max}}) \,, \tag{8.60}$$

The optimal tension T^{max} and the optimal velocity are computed numerically presuming a distribution for the crack length. For this, we have chosen the log-normal distribution. The probability density function of ξ is

$$f_\xi(x) = \frac{1}{x s_1\sqrt{2\pi}}\exp\left(-\frac{(\ln(x/c_1))^2}{2 s_1^2}\right), \quad x > 0\,, \quad s_1 > 0\,, \quad c_1 > 0\,, \tag{8.61}$$

and the cumulative distribution function is

$$F_\xi(x) = N\left(\frac{\ln x - \ln c_1}{s_1}\right), \tag{8.62}$$

where

$$N(x) = \frac{1}{\sqrt{2\pi}} \int_{-\infty}^{x} \exp\left(-\frac{t^2}{2}\right) dt \tag{8.63}$$

is the cumulative distribution function of the standard normal distribution.

8.3.2 Uncertainty in Tension

In practice, in a paper machine the tension of the plate is generated by a velocity difference between rollers. It is very likely, that for mechanical reasons, the tension practically varies lightly between minimum and maximum values i.e in-plane tension fluctuates around a given positive constant T_0. In this section, we model this phenomenon by describing the tension as

$$T \equiv T_0 + \theta \ ,$$

where θ is a random variable that has a cumulative distribution function F_θ. As before, the plate is assumed to have an initial crack of mode I. The length of the crack is assumed to be known and equal to a constant:

$$\xi = a, \quad a > 0 \ .$$

In this case, formulation of optimization problem consists of two parts. First, we seek the maximal value of T_0 satisfying

$$P(K_I \geq K_{IC}) \leq q_1 \ , \qquad \text{where } q_1 \in (0, 1) \tag{8.64}$$

is the admissible probability of fracture. Secondly, denoting the solution of inequality (8.64) by $T_0^{\max}$, we search for the maximal value of velocity V_0 under a constraint for instability:

$$P\left(V_0 > V_0^{cr}(T_0^{\max} + \theta)\right) \leq q_2 \ , \qquad \text{where } q_2 \in (0, 1) \ . \tag{8.65}$$

Here q_2 is the admissible probability of instability.

The stress intensity factor related to the crack satisfies

$$K_I = \frac{\alpha(a)\sqrt{\pi a}}{h} T = \frac{\alpha(a)\sqrt{\pi a}}{h}(T_0 + \theta) \ . \tag{8.66}$$

Noticing that

$$P(K_I \geq K_{IC}) = P\left(\theta \geq \frac{h K_{IC}}{\alpha(a)\sqrt{\pi a}} - T_0\right)$$

$$= 1 - F_\theta \left(\frac{h K_{\text{IC}}}{\alpha(a)\sqrt{\pi a}} - T_0 \right) ,$$

the constraint (8.64) is equal to

$$F_\theta \left(\frac{h K_{\text{IC}}}{\alpha(a)\sqrt{\pi a}} - T_0 \right) \geq 1 - q_1 . \tag{8.67}$$

Denote the maximal value of tension that satisfies the above inequality by $T_0^{\max}$. If the function F_θ does not depend on T_0, it is seen with similar reasoning as above that the maximal value of tension that satisfies the inequality above is

$$T_0^{\max} = \frac{K_{\text{IC}} h}{\alpha(a)\sqrt{\pi a}} - F_\theta^{-1}(1 - q_1) . \tag{8.68}$$

Furthermore,

$$P\big(V_0 > V_0^{\text{cr}}(T_0^{\max} + \theta)\big) = P\left(V_0 > \sqrt{\frac{T_0^{\max} + \theta}{m} + \gamma_*^2 \frac{\pi^2 D}{m l^2}} \right)$$

$$= P\left(\theta < m V_0^2 - T_0^{\max} - \gamma_*^2 \frac{\pi^2 D}{l^2} \right)$$

$$= F_\theta \left(m V_0^2 - T_0^{\max} - \gamma_*^2 \frac{\pi^2 D}{l^2} \right) ,$$

and we may write the inequality (8.65) as

$$F_\theta \left(m V_0^2 - T_0^{\max} - \gamma_*^2 \frac{\pi^2 D}{l^2} \right) \leq q_2 . \tag{8.69}$$

Let us denote $\theta_C = F_\theta^{-1}(q_2)$, and consider another value $\theta_C^* < \theta_C$. The two values of tension variation, θ_C and θ_C^*, satisfy $F_\theta(\theta_C) \leq q_2$ and $F_\theta(\theta_C^*) \leq q_2$. By noticing that

$$V_0 = \sqrt{\frac{1}{m} \left(T_0^{\max} + \frac{\gamma_*^2 \pi^2 D}{l^2} + \theta_C \right)} > \sqrt{\frac{1}{m} \left(T_0^{\max} + \frac{\gamma_*^2 \pi^2 D}{l^2} + \theta_C^* \right)} \equiv V_0^* ,$$

we deduce that the maximal value of V_0 satisfying (8.64) and (8.65) is

$$(V_0)_{\text{opt}} = \sqrt{\frac{1}{m} \left(T_0^{\max} + \frac{\gamma_*^2 \pi^2 D}{l^2} + F_\theta^{-1}(q_2) \right)} . \tag{8.70}$$

We assume θ to obey the truncated normal distribution with scale parameter $c_t > 0$ and location at 0. The minimum and maximum values of the distribution are set as

Table 8.8 Parameter values for numerical examples

Parameter	Value
ν	0.3
E	10^9 Pa
m	0.08 kg/m^2
h	10^{-4} m
l	0.1 m
b	5 m
G_C/ρ	10 Jm/kg

$$\theta_{\min} = -T_0 \quad \text{and} \quad \theta_{\max} = T_0 .$$

Hence, the probability function of θ is symmetrical, and expected value $E(\theta) = 0$. The cumulative distribution function of θ is

$$F_\theta(x; c_t, T_0) = \frac{N\left(\dfrac{x}{c_t}\right) - N\left(\dfrac{-T_0}{c_t}\right)}{1 - 2N\left(\dfrac{-T_0}{c_t}\right)} , \qquad (8.71)$$

where N is the cumulative distribution function of the standard normal distribution as above. In (8.70), we have

$$F_\theta(x) = F_\theta(x; c_t, T_0^{\max}) .$$

In the following, we illustrate numerically the results obtained above. The chosen parameter values are shown in Table 8.8. The paper fracture toughness K_{IC} is calculated from the equation $K_{IC} = \sqrt{G_C E}$. The value of the weight function is approximated by

$$\alpha\left(F_\xi^{-1}(1-p)\right) = \alpha(a) = 1.12 .$$

In Figs. 8.12 and 8.13 we illustrate the effect of changing the value of the distribution parameters and the admissible probability of fracture p on the optimal values, when the crack length is assumed to obey the log-normal distribution. In Fig. 8.12 the optimal tension and the corresponding optimal velocity are plotted with respect to the distribution parameters s_l and c_l of the log-normal distribution. For this, it was set $p = 0.001$.

In Fig. 8.13 we illustrate the effect of increasing the value of p from $p = 0.001$ with some values of the distribution parameters. As is expected, the optimal values increase when the admissible probability of fracture p is increased. With smaller value of s_l, the change is small. Some of the optimal values are gathered in Table 8.9.

In Fig. 8.14 we see the optimal tension and the corresponding optimal velocity plotted with respect to the distribution parameter c_t of the truncated normal
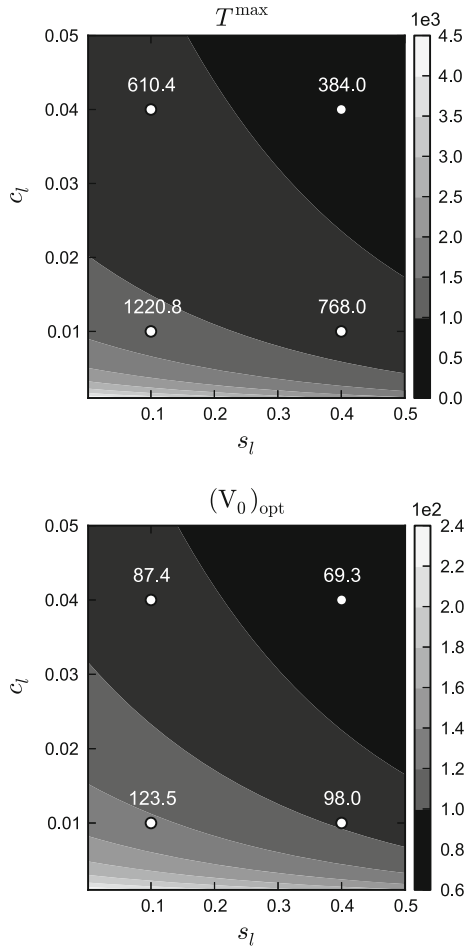
Fig. 8.12 Log-normal distribution. The effect of changing the value of the distribution parameters s_l and c_l on the optimal tension and velocity with the admissible probability of fracture $p = 0.001$

distribution. The optimal values are computed with the initial crack length $a = 0.05$. With the considered parameter values the function

$$F_\theta \left(\frac{h K_{\mathrm{IC}}}{\alpha(a)\sqrt{\pi a}} - T_0 \right) + q_1 - 1 \tag{8.72}$$

was found to be strictly decrasing with respect to T_0. The maximal value of tension was thus found by solving the equation

$$F_\theta \left(\frac{h K_{\mathrm{IC}}}{\alpha(a)\sqrt{\pi a}} - T_0 \right) + q_1 - 1 = 0 \, . \tag{8.73}$$
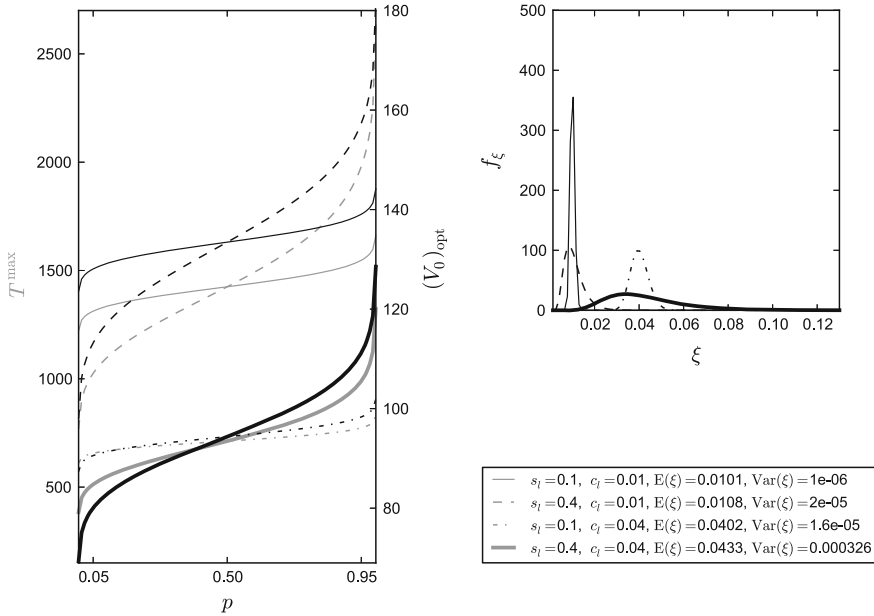
Fig. 8.13 *Left* The effect of changing the admissible probability of fracture p on the optimal values of tension and velocity, using a log-normal distribution for the crack length ξ. *Right* The probability density function of ξ

Table 8.9 The optimal tension (upper value, N/m) and velocity (*lower value*, m/s) with respect to p and the distribution parameters s_1 and c_1, using a log-normal distribution for the crack length

s_1	c_1	p		
		0.001	0.005	0.01
0.1	0.01	1,220.8	1,252.6	1,268.3
		123.5	*125.1*	*125.9*
	0.04	610.4	626.3	634.2
		87.4	*88.5*	*89.0*

Figure 8.14 shows that the more the tension is dispersed, the lower the optimal values are. Increasing the admissible probability of fracture or instability increases the optimal values. When the length of the initial crack increases, the optimal values decrease.

Some of the optimal values are gathered in Table 8.10.

To conclude, in this section we discussed the problem of finding the optimal velocity for an axially moving elastic plate with a crack from a probabilistic point of view. The model was assumed to include randomness, and the optimal velocity was investigated under the constraint that the probability of fracture is limited. Two cases were considered separately. First, the length of the crack was modelled as a random
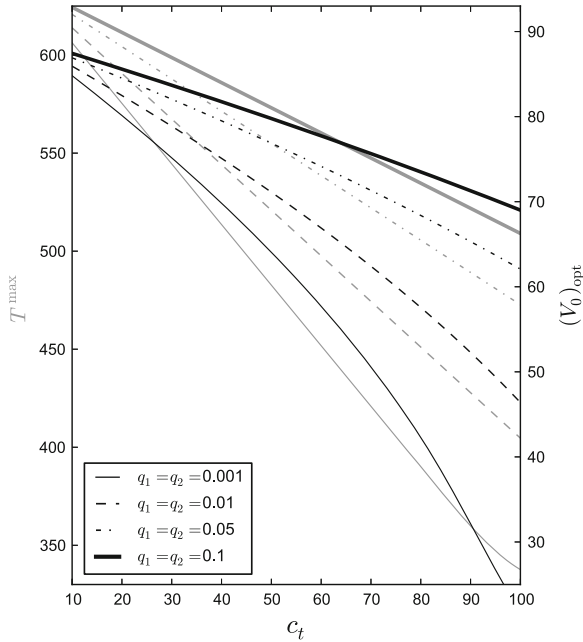
Fig. 8.14 Optimal tension and velocity, using the truncated normal distribution to model tension variation. The optimal values are shown with respect to the distribution parameter c_t, in all cases using a constant crack length $a = 0.05$. Here q_1 and q_2 are, respectively, the admissible probabilities of fracture and instability

Table 8.10 Truncated normal distribution. Optimal tensions (*upper value*, N/m) and velocities (*lower value*, m/s) with respect to the probabilities q_1 and q_2 and the distribution parameter c_t. The crack length $a = 0.05$

c_t	q_1, q_2		
	0.001	0.005	0.01
10.0	606.3	611.4	613.9
	84.8	*85.6*	*85.9*
50.0	482.7	508.4	520.9
	64.1	*68.9*	*71.1*
100.0	337.6	380.1	404.6
	21.8	*39.2*	*46.4*

variable. Secondly, the in-plane tension was assumed to be a random variable. In the latter case, we also formulated a constraint for stability.

The optimal velocity was found by first computing the optimal tension for the plate. Assuming the crack length to be random, we formulated an analytical expression for the optimal tension. Modelling the crack length with the log-normal distribution, the effect of changing the admissible probability of fracture was numerically

illustrated. It was seen that with both of the considered distributions, increasing the admissible probability of fracture increases the optimal tension and the corresponding optimal velocity.

The optimal velocity was also numerically computed for the log-normal distribution with different values of distribution parameters. The values were chosen such that the distributions were close to the presumable crack distribution of the paper making application.

The optimal tension and the related optimal velocity in the case of random in-plane tension were obtained, assuming the in-plane tension to obey a truncated normal distribution. It was seen that the more the tension is dispersed, the lower is the optimal velocity. Increasing the admissible probability of fracture had the same effect on the optimal values as in the case of random crack length. Also increasing the admissible probability of instability increased the optimal values.

References

Banichuk N, Jeronen J, Neittaanmäki P, Tuovinen T (2010) On the instability of an axially moving elastic plate. Int J Solids Struct 47(1):91–99. http://dx.doi.org/10.1016/j.ijsolstr.2009.09.020

Banichuk N, Kurki M, Neittaanmäki P, Saksa T, Tirronen M, Tuovinen T (2013) Optimization and analysis of processes with moving materials subjected to fatigue fracture and instability. Mech Base Des Struct Mach Int J 41(2):146–167. http://dx.doi.org/10.1080/15397734.2012.708630

Banichuk NV, Neittaanmäki PJ (2010) Structural Optimization with Uncertainties. Springer-Verlag, Dordrecht. ISBN 978-90-481-2517-3

Björklund KJ, Svedjebrant J (2009) Productivity improvements of a newsprint paper machine by reduction of web breaks. Master's thesis, Luleå University of Technology

Chankong V, Haimes YY (1983) Multiobjective decision making theory and methodology. Elsevier Science Publishing Co., Inc., New York

Fett T (1999) Stress intensity factors for edge-cracked plates under arbitrary loading. Fatigue Fract Eng Mater Struct 22(4):301–305. http://dx.doi.org/10.1046/j.1460-2695.1999.00156.x

Laham SA (1998) Stress intensity factor and limit load handbook. British Energy Generation Ltd., UK

Miettinen K (1994) On the methodology of multiobjective optimization with applications. Report 60, Department of Mathematics, University of Jyväskylä, ISBN 951-34-0316-5

Niskanen K (ed) (2012) Mechanics of paper products. Walter de Gruyter GmbH & Co., ISBN 978-3-11-025461-7

Paris PC, Erdogan F (1963) A critical analysis of crack propagation laws. J Basic Eng Trans Am Soc Mech Eng. D 85:528–534

Perez N (2004) Fracture mechanics. Kluwer Academic Publishers, New York

Salminen L (2003) Aspects of fracture processes in paper. PhD thesis, Helsinki University of Technology

Seth RS, Page DH (1974) Fracture resistance of paper. J Mater Sci 9(11):1745–1753. http://dx.doi.org/10.1007/BF00541741

Smith RD (1995) Roll and web defect terminology. TAPPI Press, Atlanta

Stadler W (1979) A survey of multicriteria optimization or the vector maximum problem, part I: 1776–1960. J Optim Theory Appl 29(1):1–52

Steuer RE (1986) Multiple criteria optimization: theory, computation, and applications. Wiley & Sons, Inc., New York

Uesaka T (2004) Web breaks in pressroom: a review. FSCN-rapport, FSCN, Mitthögskolan. http://books.google.fi/books?id=xs6YMQAACAAJ

Wathén R (2003) Characterizing the influence of paper structure on web breaks. Licentiate thesis, Helsinki University of Technology, Department of Forest Products Technology, espoo, Finland

White DJ (1990) A bibliography on the applications of mathematical programming multiple-objective methods. J Oper Res Soc 41(8):669–691